DNA Packaging Induced by Micellar Aggregates: A Novel in Vitro DNA Condensation System†

Rodolfo Ghirlando,‡ Ellen J. Wachtel,§ Talmon Arad,‖ and Abraham Minsky*,‡

Departments of Organic Chemistry and Structural Biology, The Weizmann Institute of Science, Rehovot 76100, Israel

Received November 19, 1991; Revised Manuscript Received March 20, 1992

ABSTRACT: Evidence for a conceptually novel DNA packaging process is presented. X-ray scattering, electron microscopy, and circular dichroism measurements indicate that in the presence of positively charged micellar aggregates and flexible anionic polymers, such as negatively charged polypeptides or single-stranded RNA species, a complex is formed in which DNA molecules are partially embedded within a micellar scaffold and partially condensed into highly packed chiral structures. Based on studies of micelle–DNA and micelle–flexible anionic polymer systems, as well as on the known effects of a high charge density upon the micellar organization, a DNA packaging model is proposed. According to this model, the DNA induces the elongation of the micelles into rodlike aggregates, forming a closely packed matrix in which the DNA molecules are immobilized. In contrast, the flexible anionic polymers stabilize clusters of spherical micelles which are proposed to effect a capping of the rodlike micelles, thus arresting their elongation and creating surfactant-free segments of the DNA that are able to converge and collapse. Thus, unlike other in vitro DNA packaging systems, in which condensation follows encounters between charge-neutralized DNA molecules, a prepackaging phase where the DNA is immobilized within a matrix is proposed in this case. Cellular and nuclear membranes have been implicated in DNA packaging processes in vivo, and negatively charged polyelectrolytes were shown to be involved in the processes. These observations, combined with the basic tenets of the DNA condensation system described here, allow for the progression to the study of more elaborate model systems and thus might lead to insights into the nature and roles of the intricate in vivo DNA–membrane complexes.

Biochemical and morphological studies have pointed toward a functional link between the eukaryotic nuclear envelope and nucleic acids (Bostock & Sumner, 1980), as well as between periplasmic membranes and the prokaryotic chromosome (Firshein, 1989). In particular, chromosome condensation during prophase has been shown to occur on the nuclear envelope (Foe & Alberts, 1983), and condensed heterochromatin regions have often been found to be closely associated with the inner nuclear membrane. It has been postulated that membranal structures, in conjunction with either acidic proteins (Adachi & Yanagida, 1989) or RNA (Nickerson et al., 1989), play an active role in DNA packaging processes during the different phases of the cell cycle (Blow & Sleeman, 1990; Leno & Laskey, 1991).

Systematic investigations of such DNA–membrane interactions are intrinsically difficult, being hindered by the necessity to isolate the labile and intricate in vivo complex. Therefore, in order to assess the potential contribution of the various factors deemed to influence nucleic acid packaging processes, experiments have been designed to try and induce the in vitro DNA condensation by membranelike systems. Initial experiments focused on the interaction of DNA with CTAB,[1] a cationic surfactant reported to interact electrostatically with DNA (Osica et al., 1977; Hayakawa et al., 1983), as well as precipitate it selectively in the presence of RNA (Morimoto et al., 1978). CTAB molecules aggregate in solution to form spherical micelles above a critical concentration referred to as the cmc [for a review see Lindmann and Wennerström (1980)], and such micellar systems represent the simplest membrane model (Fendler, 1982). In the present work we show through circular dichroism, electron microscopy, and X-ray scattering experiments that dsDNA molecules, in the presence of CTAB and an anionic polyelectrolyte, undergo a conformational transformation to yield condensed, chiral DNA tertiary structures. A thorough physicochemical study of the nature of the interaction between DNA or the accompanying polyelectrolyte with CTAB and related cationic surfactants is presented. The results of such a study enable the characterization of the properties of the condensed DNA species and lead to the proposal of a novel mechanism for in vitro DNA condensation which proceeds in a manner unlike the collapse of charge-neutralized DNA molecules (Manning, 1978). An evaluation of the model used to describe the condensation system suggests a role for the various anionic polyelectrolytes found to be required for different nuclear processes in eukaryotes. The model system described involves surfactant aggregates not found in biological systems, and thus a direct correlation with possible in vivo DNA–membrane interactions is not possible. However, the condensation mechanism allows for the progression to a study of DNA with larger surfactant aggregates, which would in turn help probe the intriguing possibility that membranal structures may be involved in the regulation of processes that depend upon the physical organization of nucleic acids, such as DNA replication and gene expression.

† This work was supported by the Fund for Basic Research administered by the Israel Academy of Sciences and Humanities.

* Author to whom correspondence should be addressed. Incumbent of the Victor L. Ehrlich Career Development Chair.

‡ Department of Organic Chemistry.

§ Chemical Services Unit.

‖ Department of Structural Biology.

[1] Abbreviations: CD, circular dichroism; cmc, critical micellar concentration; CTAB, cetyltrimethylammonium bromide; DP, degree of polymerization; DTAB, dodecyltrimethylammonium bromide; OTAB, octadecyltrimethylammonium bromide; poly-Asp, sodium polyaspartate; poly-Glu, sodium polyglutamate; TTAB, tetradecyltrimethylammonium bromide.

0006-2960/92/0431-7110$03.00/0

MATERIALS AND METHODS

Materials

Nucleic Acids. Highly polymerized calf thymus (type I, 58% AT) DNA was purchased from Sigma. The DNA was dissolved in 20 mM Tris buffer (pH = 7.5) and sonicated at 4 °C for a number of 30-s pulses using an Ultratip Labsonic system (Model 9100) sonicator from Lab-Line Instruments Inc. The DNA fragments were then loaded on a Sephacryl S-400 (Pharmacia LKB Biotechnology Inc.) column and eluted with a 20 mM Tris (pH = 7.5) and 0.25 M NaCl solution. Fractions of 5 mL were collected, and the size distribution of the DNA fragments in each fraction was determined by 0.75% agarose gel electrophoresis using λ/*Hin*dIII and *φX174*/HaeIII digestion fragments (Biolabs) as markers. The samples were extensively dialyzed against 5.0 mM Tris buffer (pH = 7.5) containing 5.0 mM EDTA and then concentrated by ultrafiltration. The average DNA size obtained depended upon the length of the sonication, and two 30-s pulses typically led to a 6000–4000 bp size distribution. DNA concentrations were determined by measuring the absorption at 260 nm using an extinction coefficient of 6600 M^{-1} cm^{-1} in terms of DNA bases (Sambrook et al., 1989). DNA lengths are reported in base pairs and concentrations in base pairs molarity. The potassium salts of poly(adenylic acid) [poly(A), mol wt > 100 000], poly(guanylic acid) [poly(G), mol wt > 150 000], poly(uridylic acid) [poly(U), mol wt > 100 000] and poly(adenylic acid)·poly(uridylic acid) [poly(A)·poly(U)] were purchased from Sigma.

Polypeptides. The sodium salts of poly(L-glutamic acid) (DP = 88, 163, 285, 490, and 515), poly(D-glutamic acid) (DP = 130, 135, 380, and 630), poly(DL-glutamic acid) (DP = 120), and poly(L-aspartic acid) (DP = 53 and 120) were purchased from Sigma. The concentrations are reported in amino acid molarities.

Surfactants. Dodecyltrimethylammonium bromide (DTAB, 99%) was purchased from Aldrich, tetradecyltrimethylammonium bromide (TTAB, 99%) was purchased from Sigma, and cetyltrimethylammonium bromide (CTAB, 98%) was obtained from BDH, and these surfactants were used as is.

Synthesis of Octadecyltrimethylammonium Bromide. 1-Octadecylamine (10.0 g, 37.1 mmol) was mixed with 18.0 mL (74.2 mmol) of *n*-tributylamine and 50 mL of dried dimethylformamide, all under an inert argon atmosphere. This was treated with an excess of methyl bromide and allowed to stir at 40 °C under a dry-ice condenser. After 1 week, the mixture was cooled to 4 °C and the resulting precipitate was collected and washed with water followed by 95% EtOH, absolute EtOH, and diethyl ether. The resulting dry white solid was recrystallized twice from hot tetrahydrofuran to yield 3.20 g (22% yield) of a white solid which melted above 200 °C (lit. mp (Shelton et al., 1946) 230–240 °C). This gave a satisfactory NMR spectrum (Bruker WH 270 MHz, $CDCl_3$): δ = 3.57 (m, 2 H), 3.50 (s, 9 H), 1.83 (m, 2 H), 1.26 (m, 30 H), 0.93 (t, J = 7.7 Hz, 3 H).

Methods

UV absorption spectra were recorded on a Hewlett-Packard 8450A diode array spectrophotometer using 1.0-cm path length quartz cuvettes. All of the measurements were carried out at room temperature (20–24 °C). The samples were prepared by mixing the required amounts of the various stock solutions. In the case of the cationic surfactant induced DNA condensation, this order of addition was followed: DNA, the accompanying polyelectrolyte, water, surfactant, and EtOH. Other samples were prepared in a similar fashion. All of the solutions were prepared using unbuffered solutions as it was noted that the buffer salts suppressed the large $\Delta\epsilon$ values obtained by CD spectroscopy. The solutions had pH values ranging from 6.9 to 7.5, uncorrected for the presence of either the surfactant or the added EtOH. The EtOH concentration is given as a volume/volume percentage and is uncorrected for volume contractions due to mixing.

Circular Dichroism. Circular dichroism spectra were recorded on a Jasco J-500C spectropolarimeter equipped with a DP-500N data processor. Studies on condensed DNA were executed using either 0.1- or 1.0-cm path length quartz cells. As the CD spectra of compact nucleic acid structures are usually hard to reproduce accurately (Keller & Bustamante, 1986b), each experiment was repeated at least three times on independent samples. The spectra reported in all figures are representative and it should be noted that for identical mixtures only the absolute magnitude of the CD spectrum exhibits a narrow variability; the shape and sign of the spectra are fully reproducible. All spectra were recorded 5 min following the addition of the alcohol.

Fluorescence Polarization. Fluorescence polarization measurements were carried out with an instrument based on the description of Weber and Bablouzian (1966). The exciting beam (365 nm) was generated from a 500-W mercury arc lamp and passed through a Heath EU-700 monochromator followed by a Glan-air polarizer which can be fixed accurately in a horizontal or vertical position. The emission was analyzed simultaneously on two independent cross-polarized channels at right angles to the incoming excitation beam. In the reference channel, the emission is observed through a horizontally oriented Glan-Thompson polarizer followed by a cutoff filter which eliminates scattering artifacts. A vertically oriented Glan-Thompson polarizer is used for the emission channel, followed by a cutoff filter. The ratio of the fluorescence intensities detected in the emission and reference channels can be correlated to the microviscosity around the fluorescent probe (Shinitzky et al., 1971).

Electron Microscopy. Samples for electron microscopy were prepared by applying 10 μL of the solutions on the carbon side of untreated carbon-coated grids (400 mesh) for 30 s, followed by removal of the excess solution with filter paper. The specimen was immediately stained by the application of a 1% (w/v) aqueous uranyl acetate solution for 30 s. The grid was then blotted with filter paper and air dried. As in the case of the CD spectroscopy samples, the EtOH was added just prior to sample preparation for the condensed DNA systems. Samples in which the interaction of polyelectrolytes with surfactants were studied were allowed to equilibrate to 19 °C for 30 min. The sample grids were then prepared in the usual manner. Specimens were examined on a Phillips EM400-T electron microscope operating at 100 kV. Specimens from three independently prepared identical samples were examined to rule out possible artifacts, and the figures shown exhibit typical structures which were observed reproducibly. Electron micrographs of the ordered surfactant polyelectrolyte domains were examined on an optical diffractometer.

X-ray Scattering. The instrumentation for both the small- and wide-angle X-ray scattering measurements has been described in a previous communication (Wachtel et al., 1991). Anhydrous cholesterol and calcite were used as calibrating materials. For low-angle scattering from polyelectrolyte–

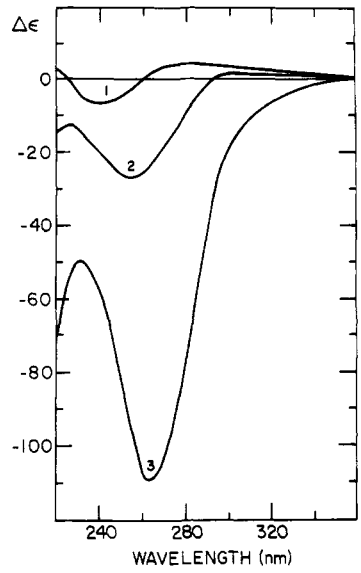

FIGURE 1: Effect of different cationic surfactants on DNA condensation: CD spectra of Ψ⁻-DNA aggregates induced by different cationic surfactants. The spectra were obtained under the following sample conditions: DNA (50 μM, 9500–4000 bp), poly(L-Glu) (50 μM, DP = 285), 25% aqueous EtOH, and 50 mM of the following surfactants: (1) DTAB, (2) TTAB, and (3) CTAB. In the case of OTAB a spectrum of B-DNA as shown in Figure 3 is obtained. Largest absolute values of $\Delta\epsilon_{265}$ are observed for CTAB.

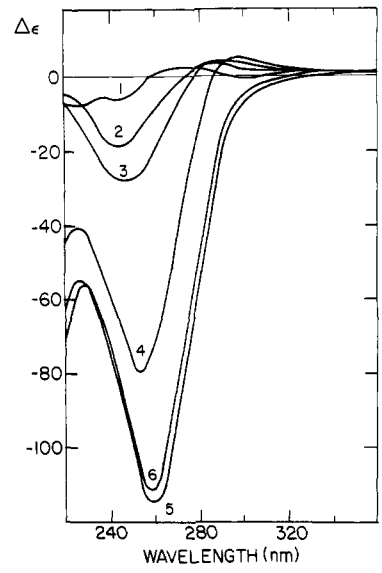

FIGURE 2: Effect of the CTAB concentration upon the Ψ⁻-DNA condensation processes. The spectra were obtained under the following sample conditions: DNA (50 μM, 9500–4000 bp), poly-(L-Glu) (50 μM, DP = 285), 25% aqueous EtOH, and the following concentrations of CTAB: (1) 10 mM, (2) 20 mM, (3) 30 mM, (4) 40 mM, (5) 50 mM, and (6) 60 mM. No condensation is observed below 10 mM CTAB.

surfactant mixtures, the samples were flame-sealed in 1.5-mm-diameter lithium-glass X-ray capillaries. Data acquisition times were 6 h for DNA-containing samples and 24 h for those samples which contained polypeptides. In the case of condensed DNA, pellets were prepared by gentle centrifugation (1000 rpm for 30 min on a table-top centrifuge with a rotor radius of 15 cm) of 50-mL solutions containing the same concentrations of the various constituents as samples typically prepared for CD spectroscopy. Data acquisition time for DNA condensate samples was 24 h at 15 °C. The resulting films were analyzed using a Joyce-Loebl microdensitometer.

RESULTS

(*A*) *DNA–Polyelectrolyte–Surfactant Systems.* When treated with sodium poly(L-glutamate) [poly(L-Glu)] and CTAB in 25% aqueous EtOH, DNA molecules undergo condensation to yield structures in which the closely packed DNA helices assume a left-handed tertiary organization, as evidenced by the large negative nonconservative CD signals (Figure 1). Such spectra, coined Ψ⁻, are known to characterize packed DNA species (Maestre & Reich, 1980; Bustamante et al., 1983; Keller & Bustamante 1986a,b; Kim et al., 1986). A surfactant was found to be necessary for the DNA condensation, as CD studies show that tetramethylammonium bromide (TMAB) in the presence of poly(L-Glu) and 25% aqueous EtOH does not elicit condensation. In this case a conservative spectrum characteristic of B-DNA is obtained. The absence of DNA condensation in the presence of TMAB was further confirmed by electron microscopy, in which no DNA aggregates were observed, as well as by X-ray scattering experiments.

In order to characterize the requirements for this CTAB-induced DNA condensation, a series of trimethylammonium surfactants ranging from DTAB through to OTAB were investigated. As noted in Figure 1, TTAB and CTAB lead to Ψ⁻ CD signals, indicating the formation of a chiral DNA condensate, whereas DTAB and OTAB do not. OTAB does not form micellar aggregates, and the fact that this surfactant fails to elicit DNA condensation in the presence of poly(L-Glu) suggests that the ability of the surfactant to aggregate into micelles is required for DNA packaging. This notion is supported by the findings that no DNA condensation can be observed below the cmc (Figure 2). Significantly, the solvent system in which packaging occurs (i.e., 25% aqueous EtOH) does not interfere with micellization, as evidenced by X-ray scattering, in which radii of gyration corresponding to spherical micellar diameters of 31 ± 1 Å and 27 ± 1 Å were measured for CTAB in water and 25% aqueous EtOH, respectively (Ghirlando, 1991). The facts that condensation is observed for TTAB and CTAB but not DTAB and that the micellar size increases with the surfactant chain length indicate some form of tuning between the size and nature of the surfactant aggregate (Israelaschvili, 1985) and the extent of DNA condensation.

CD spectra of the DNA molecules in the presence of TTAB and CTAB, obtained under conditions which do not induce chiral packaging [i.e., in the absence of either poly(L-Glu) or EtOH] exhibit an attenuated positive lobe at 280 nm, an increased negative lobe at 245 nm, and a red shift of the crossover point (Figure 3). Such spectral modulations, indicative of secondary conformational perturbations (Ivanov et al., 1973; Saenger, 1984), are not observed in the presence of either DTAB or OTAB, pointing toward a possible correlation between DNA packaging processes and surfactant-induced modifications within the nucleic acid's secondary structure. Notably, the spectral changes do not depend upon the solvent used, being water or 25% aqueous EtOH, and in the case of aqueous surfactant solutions, they are not affected by the presence of poly(L-Glu).

The DNA secondary conformation within the DNA condensate obtained with poly(L-Glu) and CTAB in 25% aqueous EtOH was studied by wide-angle X-ray scattering. Based on a comparison of the data obtained experimentally (Table I) and that calculated for DNA oligomers (Maniatis, 1971), an overall B-DNA secondary structure is assigned to the condensed DNA. The absence of a scattering peak (or shoulder) at 8.7 Å would, however, suggest structural perturbations in the B-DNA secondary structure. The

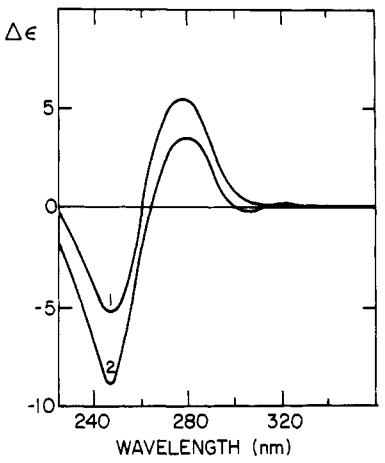

FIGURE 3: DNA secondary conformation with different cationic surfactants: the CD spectra of DNA in the presence of different surfactants. The samples contained DNA (50 μM, 4500–1500 bp) and 50 μM of the surfactant indicated: (1) DTAB or OTAB; (2) TTAB or CTAB. Similar results were noted in the presence of either poly(L-Glu) (DP = 285) or 25% aqueous EtOH.

scattering peak observed at 7.6 Å characterizes the CTAB surfactant, as a scattering peak at 7.6 Å is noted for CTAB solutions, and the peak at 4.2 Å is assigned to scattering from the dsDNA helices. The peak observed at 25 Å is assigned to the close packing of the dsDNA helices within the Ψ⁻-DNA condensate. Assuming a hexagonal lattice for the close-packed DNA (Schellman & Parthasarathy, 1984; Maniatis et al., 1974), this corresponds to a DNA–DNA interhelical distance of 28.9 Å and a chromophore density of 0.81 chromophores/nm^3.

Ψ⁻-DNA condensation is induced in the presence of poly(L-Glu) and CTAB in 25% aqueous EtOH. The polyelectrolyte is necessary for the DNA condensation, as in its absence no Ψ⁻-CD spectrum characteristic of the condensed DNA states is noted and the 25-Å scattering peak arising from the close packing of the DNA helices is no longer observed. In addition, no condensation is observed when the poly(L-Glu) is replaced by the monomer sodium L-glutamate, further emphasizing the requirement of a polyelectrolyte. In order to assess the role of the anionic polyelectrolyte in the condensation process, the effects of three factors, size, chirality, and flexibility of the negatively charged polymers, were investigated. The various poly-Glu species studied can be divided into two classes depending upon the size of the nonconservative CD signal exhibited by the DNA condensates. Class I induces large CD signals and includes the relatively short polyelectrolytes (DP = 88–285 residues), whereas class II, consisting of the longer poly-Glu species (DP = 380–630), leads to relatively attenuated $\Delta\epsilon_{265}$ values. The difference between the two classes is further indicated by titration experiments (Figure 4). As the class I polyelectrolyte concentration is increased beyond the optimal value of 50 μM, the large CD signals revealed by the DNA condensates decrease rapidly to zero. In contrast, the concentration-dependent decrease of the nonconservative ellipticities induced by class II is substantially slower. These data suggest that the DNA condensation process is sensitive to both the molar ratios of DNA base pairs to the negative charges on the polyelectrolytes and the total number of polyelectrolyte molecules. Nonconservative CD signals are also obtained when poly(L-Glu) is replaced by sodium polyaspartate (poly-Asp) of a similar length or by the ribonucleic acids poly(A) or poly(U), indicating that these species are capable of inducing DNA condensation within the DNA–anionic polymer–surfactant system. Yet, the intensity of the nonconservative ellipticities obtained in those cases is significantly attenuated. The difference between poly-Glu and poly-Asp lies in the spacer separating the carboxylate group from the backbone, being shorter for the poly-Asp. The ribonucleic acids are characterized by a higher degree of rigidity than the polypeptides. Thus, the efficiency of the condensation process is suggested to correlate with the degree of the conformational flexibility of the polyelectrolyte, as well as the flexibility of the tethered anionic groups. Indeed, when the particularly rigid poly(G) (Barr & Pinnavaia, 1986) and the duplex poly(A)·poly(U) are used as polyelectrolytes, no DNA condensation is observed. Finally, the properties of the DNA condensates are found to be independent of the chirality of the polyelectrolyte, and a poly(DL-Glu) random polymer leads to CD patterns identical to those induced by poly(L-Glu) or poly(D-Glu) of similar length.

The nonconservative CD signals revealed by the condensed DNA species exhibit a red shift and decreased intensities as the DNA concentration within the packaging system is increased (Figure 5). These data indicate that the condensation process is one of intermolecular DNA aggregation, as opposed to an intramolecular collapse mechanism, as both the red shift in λ_{max} and the decrease in the absolute value of $\Delta\epsilon_{265}$ can be assigned to the presence of larger aggregates. In order to further examine the nature of the proposed intermolecular condensation process, different lengths of DNA were prepared by sonication and their condensation induced by poly(L-Glu) and CTAB was investigated by CD spectroscopy. DNA molecules having a size in the range of 9500–500 base pairs exhibit similar values of $\Delta\epsilon_{265}$, indicating that the condensation process is relatively insensitive to the DNA size. Notably, DNA as short as 100–20 base pairs still gives rise to a characteristic Ψ⁻ CD spectrum, an observation which is incompatible with an intramolecular packaging process or with the formation of curved DNA condensates, in which a critical minimum length of the DNA is required (Marquet et al., 1987; Arscott et al., 1990).

Electron microscopy studies performed on the DNA–CTAB–polyelectrolyte systems indicated the reproducible formation of aggregates whose morphology depended upon the size of the DNA molecules. The long DNA molecules (9500–4000 bp) yielded aggregates characterized by a thick filamentous structure with a diameter of approximately 300 Å (Figure 6A). Such a morphology is reminiscent of the structure of DNA condensates obtained at high EtOH concentrations (Lang, 1973; Eickbush & Moudrianakis, 1978). In the case of the shorter DNA molecules (Figure 6B), less well defined aggregates associated with some form of substructure were noted. The overall size of the aggregates were found to depend solely upon the CTAB concentration, with larger particle sizes being observed as the surfactant concentration is increased. Notably, similar aggregates were obtained in the absence of the anionic polyelectrolytes, indicating that the observed structures represent a DNA–surfactant complex, whose gross morphology is not affected by the anionic polymer. The quantity of the aggregates was found, however, to depend upon the molar ratio between the flexible polyelectrolyte and the DNA; at large molar ratios the number of the aggregates was observed to decrease and at a ratio of 10/1 (amino acids or nucleotides to base pairs) no such particles could be detected.

(B) Polyelectrolyte–Cationic Surfactant Systems. Aggregates of the forms depicted in Figure 6 could not be detected in samples containing CTAB and poly(L-Glu), but not DNA,

Table I: DNA Secondary Conformation by Wide-Angle X-ray Scattering[a]

DNA	DNA–DNA d_B	peak (Å)					
		1	2	3	4	5	6
Ψ⁻-DNA	25 ± 2	12.8 ± 0.4	7.6 ± 0.2[b]	5.4 ± 0.2	4.2 ± 0.2	3.8 ± 0.1	3.4 ± 0.1
A-DNA		12.50	7.45	5.33	4.13	3.55	3.24
B-DNA		12.59	8.69	5.33	4.26	3.83	3.29
C-DNA		11.42		5.33	4.13	3.53	3.30

[a] The Ψ⁻-DNA pellets were prepared by gentle centrifugation of solutions containing DNA (50 μM, 6500–2000 bp), poly(L-Glu) (50 μM, DP = 285), CTAB (50 mM), and 25% aqueous EtOH. The pellet was placed in a 1.5-mm-diameter glass capillary and studied at 15 °C. The numbering of the peaks follows from Maniatis et al. (1974), from which the scattering data calculated for oligomers of A, B, and C-DNA were obtained. The data are an average of three determinations and the error reflects the standard deviation from the mean. [b] This peak arises, at least in part, from the CTAB–CTAB interactions and does not reflect a DNA scattering contribution. It is also observed for CTAB solutions. No shoulder or peak is noted at 8.7 Å.

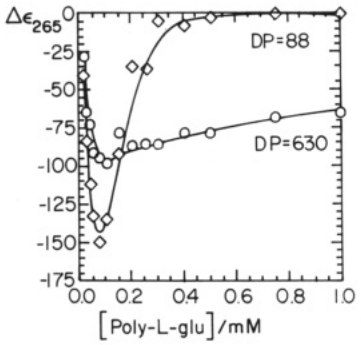

FIGURE 4: Effect of polyelectrolyte size and concentration: effect of the length and concentration of poly-Glu upon the DNA condensation. The titration experiments illustrate the behavior of the two classes of polyelectrolytes discussed (i.e., class I, poly(L-Glu), DP = 88, and class II, poly(D-Glu), DP = 630). The samples contained DNA (50 μM, 9500–4000 bp), poly-Glu as indicated, CTAB (50 mM), and 25% aqueous EtOH. The data are the mean of two determinations.

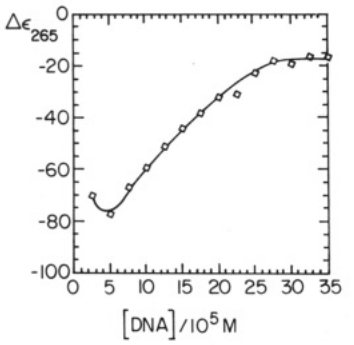

FIGURE 5: Intermolecular condensation: comparison of the effect of the DNA concentration upon Ψ⁻-DNA condensation. The samples contained the indicated amount of DNA (4000–800 bp), poly(L-Glu) (50 μM, DP = 515), CTAB (50 mM), and 25% aqueous EtOH. The data shown are the result of one experimental determination.

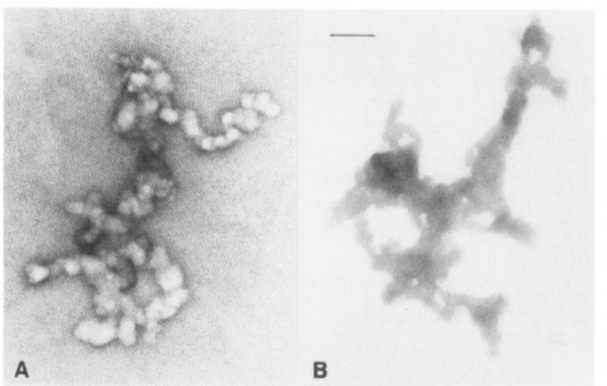

FIGURE 6: Morphology of Ψ⁻-DNA: electron microscopy of condensed DNA structures obtained in the presence of CTAB and EtOH. The samples contained DNA (50 μM), poly(L-Glu) or poly(L-Asp) (50 μM), CTAB (30 mM), and 25% aqueous EtOH. The following DNA lengths and polyelectrolytes were considered: (A) 9500–4000 bp, poly(L-Glu) DP = 285; (B) 1000–100 bp, poly(L-Asp) DP = 120. Note that whereas the specimen in panel A is negatively stained, the condensed structure in panel B appears as positively stained. Although the reason for such a difference is not clear, it may be suggested that the aggregate depicted in (A) is more tightly packed than that in (B), leading to a higher degree of exclusion of the stain. The scale bar represents 1000 Å.

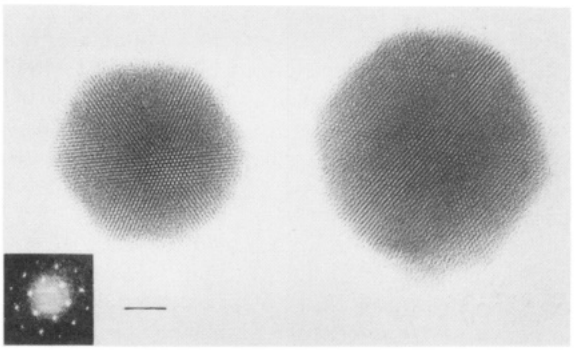

FIGURE 7: Surfactant assembly: electron microscopy of negatively stained microcrystalline domains formed between polyelectrolytes and cationic surfactants in 25% aqueous EtOH. The samples contained poly(L-Asp) (50 μM, DP = 120), CTAB (30 mM), and 25% aqueous EtOH. The scale bar represents 500 Å. The inset shows the optical diffraction resulting from the micrograph for the microcrystalline domain shown on the left. The first-order diffraction spacing corresponds to 40.0 Å.

further buttressing the notion that these structures are indeed DNA aggregates. Yet, samples containing CTAB and poly(L-Glu) revealed the presence of hexagonally shaped organized domains, characterized by a hexagonal symmetry (Figure 7). A study of the conditions leading to the observation of such ordered domains points toward a clear correlation between the properties of the polyelectrolyte required for the formation of these domains and those which lead to Ψ⁻-DNA condensation. Thus, poly-Glu, poly-Asp, and poly(A) induce the CTAB surfactant organization, whereas poly(G), poly(A)·poly(U), and sodium L-glutamate do not. As shown in Table II, the spacing characterizing this quasihexagonal order is independent of the concentration and size of the polyelectrolyte. The size of the microcrystalline domains was also found to be independent of the polyelectrolyte concentration, even at concentrations as high as 1.0 mM. The quantity of such domains observed on the grid is, however, directly proportional to the polyelectrolyte concentration, and it was noted that the shorter polyelectrolytes led to a larger number of ordered domains when compared to the longer polymers. The longer polyelectrolytes give rise to an appreciable number of ordered domains only at high concentrations, and on the basis of this behavior the polyelectrolytes can be classified

Table II: Characteristic Spacing for Micellar Assembly[a]

polyelectrolyte	DP	concn (μM)	diffraction spacing (Å)	no. of domains[b]	std deviation[c] (Å)
poly(L-Glu)	88	50	39	22	2.0
poly(D-Glu)	135	50	37	13	2.4
poly(L-Glu)	285	50	38	52	2.4
poly(D-Glu)	630	50	40	1	–
poly(L-Asp)	53	25	40	10	0.7
poly(L-Asp)		50	41	12	1.3
poly(L-Asp)		100	40	7	0.6
poly(L-Asp)		250	40	13	0.8
poly(L-Asp)	120	50	40	30	1.6
poly(A) RNA	>500	50	41	4	0.8

[a] The samples contained, in addition to the polyelectrolyte indicated, CTAB (30 mM) and 25% aqueous EtOH. The samples were prepared in the manner described under X-ray Scattering. The diffraction spacing reported is the average based on the number of domains given. [b] This is the number of individual micrographs which were used in the study and fulfilled the criteria discussed in the Materials and Methods section. [c] Note that the overall standard deviation is lower when poly(L-Asp) is used as the polyelectrolyte, demonstrating the improved order which this anionic polymer induces.

into the same two classes described earlier. Significantly, no ordered structures could be observed in the absence of the polyelectrolyte. Another correlation to the Ψ^--DNA condensation is noted from the fact that such organized domains are observed only for TTAB and CTAB but not for DTAB and OTAB. The TTAB gives rise to an array having a characteristic diffraction spacing of 37.5 ± 0.5 Å, which is smaller than that obtained for CTAB. The morphology and fine structure of the organized domains indicates that they consist of a two-dimensional arrangement of spherical micelles, and the diffraction spacing of 40 Å noted for the CTAB micellar order corresponds to a micelle–micelle distance of 46 Å within this two-dimensional hexagonal symmetry.

In order to better understand the nature of the polyelectrolyte-induced surfactant organization observed by electron microscopy, fluorescence polarization and X-ray scattering studies were carried out. *N*-Hexadecyl-1-naphthylaminesulfonate was selected as the fluorescent probe as, being incorporated within the surfactant aggregate with its fluorescent aromatic head group appropriately positioned on the hydrophilic surface, it is expected to provide data on the microenvironment surrounding the aggregate. For 50 mM aqueous solutions of TTAB and CTAB, but not of DTAB, the microviscosity around the micelles is observed to increase with an increasing poly(L-Glu) concentration, an increase which can be assigned to an enhanced surfactant bulk organization. A correlation between the fluorescence measurements and the EM results is, consequently, pointed out. Similar experiments conducted in 25% aqueous EtOH indicated that in this solvent system a higher concentration of poly(L-Glu) was required to induce an increase in the microviscosity.

The samples which exhibited the highest microviscosity were studied by X-ray scattering, in order to obtain structural information concerning the polyelectrolyte-induced bulk surfactant organization. The samples which led to surfactant organization, as evidenced by fluorescence polarization, showed a single scattering peak and the results obtained are summarized in Figure 8, as a plot of the spacing (d) against the surfactant chain length n. In the case of 25% aqueous EtOH solutions the spacing is found to be linearly dependent upon n and the best-fit straight line is given by

$$d = 18 + 1.4n \qquad (r = 0.984) \qquad (1)$$

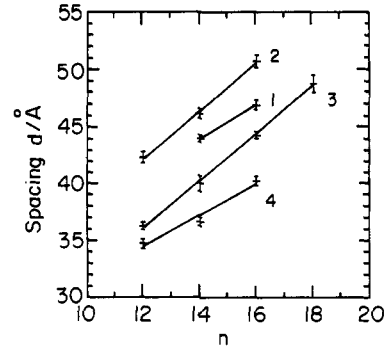

FIGURE 8: Polyelectrolyte-induced surfactant organization: X-ray scattering peaks observed for samples of poly(L-Glu) or poly(D-Glu) or DNA with different surfactants as a function of their chain length n. The samples contained (1) poly(L-Glu) (1.0 mM, DP = 285) in H_2O, (2) DNA (2.0 mM, 6500–2000 bp) in H_2O, (3) DNA (2.0 mM, 6500–2000 bp) in 25% aqueous EtOH, and (4) poly(D-Glu) (10 mM, DP = 380) in 25% aqueous EtOH and 50 mM of the trimethylammonium bromide surfactant indicated. The data shown are the average of at least three determinations and the error bars reflect the standard error of the mean.

In aqueous solution the straight line describing the two data points is given by

$$d = 24 + 1.4n \qquad (2)$$

This linear dependence upon the surfactant chain length implies that the slope reflects the contribution of the hydrophobic chains to the spacing and that this contribution does not depend upon the solvent used. Significantly, the spacings observed in 25% aqueous EtOH are identical to those observed by EM for the microcrystalline ordered micellar domains of CTAB (40.4 Å) and TTAB (37.5 Å), suggesting that a similar surfactant organization is being observed, that is, an organized micellar cluster stabilized by poly(L-Glu). A direct correlation between the microviscosity values derived from fluorescence polarization and the intensity of the scattering peak could be made. Notably, no scattering peaks were observed in the absence of either the polyelectrolyte or the surfactant, as well as when sodium L-glutamate replaced poly(L-Glu) in the samples. The positions of the scattering peak were not dependent upon the type, length, or concentration of the polyelectrolyte.

(*C*) *DNA–Cationic Surfactant Systems.* The conspicuous difference in the morphology of the species shown in Figures 6 and 7 (DNA–CTAB and poly(L-Glu)–CTAB complexes, respectively) indicates that DNA induces a different kind of surfactant organization from that effected by poly-Glu. This result is further pointed out by X-ray scattering studies. As in the case of the poly(L-Glu)-induced surfactant organization, a linear dependence of the Bragg scattering peak upon the surfactant length was noted (Figure 8, lines 2 and 3). The best-fit straight lines for the DNA-induced organization are given by

$$d = 11 + 2.1n \qquad (r = 0.999) \qquad (3)$$

in 25% EtOH and

$$d = 16 + 2.1n \qquad (r = 0.999) \qquad (4)$$

in water. The notion that different forms of surfactant organization are induced by DNA and poly-Glu follows from the different dependence of the scattering peak upon the surfactant chain length, which is manifested by the different slope of lines 2 and 3 versus that characterizing lines 1 and 4 (Figure 8). In addition, a carbon-chain contribution of 33.6 Å is obtained in the case of CTAB, a value that is larger than the micellar diameter, thus demonstrating that the observed

Table III: Ψ⁻-DNA Condensation[a]

surfactant	surfactant organization[b] (Å)	DNA–DNA peak[c] (Å)
DTAB	36 ± 1	
TTAB	40 ± 1	22.5 ± 0.4
CTAB	44 ± 1	25.4 ● 0.4

[a] The DNA pellets were prepared by gentle centrifugation of samples containing DNA (50 μM, 4000–800 bp), poly(D-Glu) (50 μM, DP = 380), 50 mM of the surfactant indicated, and 25% aqueous EtOH. [b] This X-ray peak arises from the DNA-induced surfactant organization within the pellet. Such peaks are also obtained by direct mixing of the DNA with the surfactant as shown in Figure 10. [c] This X-ray peak arises from DNA–DNA packaging and is not observed for DTAB or when the pellets are prepared in the absence of poly(D-Glu). The data are the mean of three determinations and the error represents the standard deviation from the mean. In the case of CTAB, the data are the average of six determinations, and for all of the surfactants shown, the peak position is not dependent upon the DNA base pair composition.

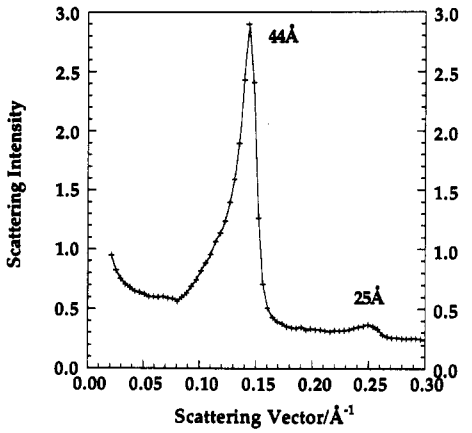

FIGURE 9: X-ray scattering profile for Ψ⁻-DNA. The DNA pellet was prepared by gentle centrifugation of a solution containing DNA (50 μM, 6500–2000 bp), poly(L-Glu) (50 μM, DP = 285), CTAB (50 mM), and 25% aqueous EtOH. The peaks at 44 Å reflects the contribution of the DNA–CTAB complex, whereas the peak at 25 Å arises from the DNA–DNA close packaging. This peak is absent when poly(L-Glu) is not included in the sample.

phenomenon is not due to a spherical micellar aggregation. Furthermore, X-ray scattering measurements performed on DNA–OTAB complexes reveal a Bragg peak which correlates linearly with the data observed for the other cationic surfactants (Figure 8). As OTAB is incapable of forming spherical micelles, a different type of organization from that induced by the flexible anionic polyelectrolyte must be assumed for all DNA–surfactant complexes.

Pellets of condensed DNA species, obtained in the presence of poly-Glu, EtOH, and TTAB or CTAB reveal a 25-Å scattering peak characteristic of DNA–DNA close packaging, in addition to the scattering peaks which reflect the DNA–surfactant clustering and depend upon the surfactant's length (Table III, Figure 9). The 25-Å peak is not observed when TTAB or CTAB is replaced by DTAB or when the DNA pellets are prepared in the absence of poly-Glu, thus providing a direct link between DNA packaging and the Ψ⁻-CD signals.

DISCUSSION

Surfactant Organization Induced by Conformationally Flexible Anionic Polyelectrolytes. The anionic polyelectrolytes such as poly(L-Glu) and DNA bind cationic surfactants in solution. The binding, driven principally by electrostatic attractive forces, is cooperative due to the hydrophobic association of the surfactant chains. The literature reports describing polyelectrolyte–surfactant interactions have focused on the measurement of the binding constant K and the cooperativity parameter u, at surfactant concentrations below the cmc (Hayakawa et al., 1983; Goddard, 1986b; Shirahama et al., 1982). Above the cmc, micellar aggregates represent the thermodynamically stable species (Israelaschvili, 1985) and it is expected that the interaction of the polyelectrolyte with the surfactant will be influenced by the stability of the micellar aggregate. The EM observations reported in this study indicate that conformationally flexible anionic polyelectrolytes stabilize the formation of ordered clusters of spherical micelles. The presence of such an organization in solution has also been indicated by fluorescence polarization and X-ray scattering experiments. The fact that the X-ray spacings observed for TTAB and CTAB with the various anionic polyelectrolytes, in 25% aqueous EtOH solutions, are identical to the diffraction spacing characterizing the two-dimensional hexagonal microcrystalline domains observed by EM suggests that a similar kind of order is noted in the bulk. Therefore, the bulk surfactant organization is proposed to arise from clusters of closely packed spherical micelles stabilized by the interweaving flexible polyelectrolytes.

Using the relations between the X-ray spacing and the surfactant chain length described in eqs 1 and 2, it is possible to calculate the micellar size within the cluster, assuming a close packing and based on the $1.4n$ contribution of the surfactant chain combined with a knowledge of the size of the head group. Neutron scattering experiments on TTAB micelles show that the trimethylammonium head group has an effective thickness of 2.0 Å (Tabony, 1984). Therefore the micellar diameter within the cluster is given by $4.0 + (2/\sqrt{3})1.4n$, or 30 Å for CTAB, which corresponds reasonably well to the value of the CTAB micellar diameter observed in aqueous solution and is just larger than that observed in 25% aqueous EtOH. Thus, the micellar size within the cluster is comparable to the micellar size in solution. Thus, in combination with the observation that an identical surfactant organization is induced by a variety of flexible anionic polyelectrolytes, indicates that the observed organization is dominated by the intermicellar interactions. Indeed, the observation that the X-ray spacing decreases on going from aqueous to 25% aqueous EtOH is consistent with this notion, as is the observation that surfactant organization is noted for TTAB and CTAB but not for DTAB in aqueous solution. This presumably follows from the reports in which the second virial coefficient characterizing the intermicellar interactions is similar for TTAB and CTAB (Imae et al., 1985), yet smaller for DTAB (Imae & Ikeda, 1986), hence indicative of decreased intermicellar interactions for DTAB. In summary, the anionic polymer serves as a nucleus for spherical micellar clustering in a manner similar to the "beads on a string" model proposed for the interaction between flexible uncharged polymers and anionic surfactants (Goddard, 1986a). According to this model, systems composed of micelles and flexible polymers are significantly stabilized by the looping of the polymer around the micelles, as such looping acts to reduce unfavorable inteactions between water molecules and methylene groups partially exposed on the micelle's surface.

Surfactant Organization Induced by DNA. DNA also interacts with the cationic surfactants studied; however, unlike the case of the flexible polyelectrolytes, the induced surfactant organization is inconsistent with the formation of hexagonally close-packed spherical micelles, as evidenced by both EM and X-ray scattering. The differences presumably arise from the fact that DNA is a more rigid macromolecule than the polypeptides studied or single-stranded RNA species.

The B-form of DNA has a radius of 10 Å and a helical rise of 3.4 Å per two phosphate groups, which implies a surface

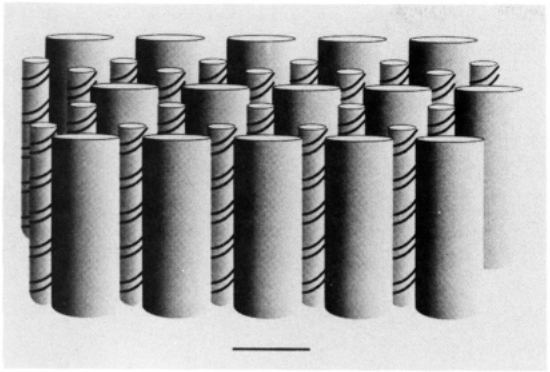

FIGURE 10: DNA-induced surfactant organization I: an idealized representation of the DNA-induced rodlike micellar organization shown in elevation for DNA and CTAB in aqueous solution. CTAB is represented as a broad rod, while the DNA is represented by the striped rods. Note the hexagonal arrangement. The diagram is approximately to scale with the scale bar representing 50 Å.

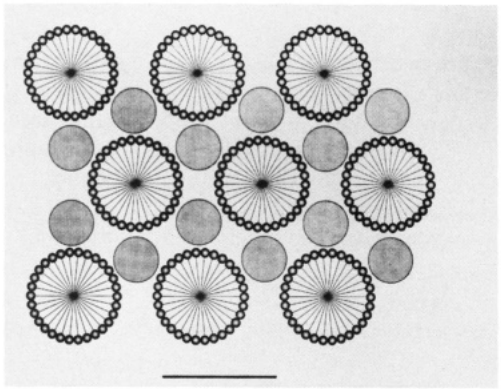

FIGURE 11: DNA-induced surfactant organization II: an idealized representation of the DNA-induced rodlike micellar organization shown in cross section. The DNA is shown in cross section as a filled grey circle, while the rod-like micelle is shown in cross-section as an aggregate of single surfactant molecules. The diagram is approximately to scale with the scale bar representing 50 Å.

area of 107 Å^2 per phosphate. Considering a coaxial cylinder of 17 Å around the DNA (Riemer & Bloomfield, 1978; Manning, 1979), then the volume corresponding to a 7-Å distance from the surface of the dsDNA helix contains a local phosphate concentration of 1.65 M. It has been reported that above a critical NaBr concentration (indicated in parentheses) solutions containing micelles of DTAB (1.8 M) (Ozaki & Ikeda, 1982) TTAB (0.12 M) (Ozaki & Ikeda, 1982), and CTAB (0.06 M) (Imae et al., 1985) exhibit the formation of rod-like micelles. Therefore, the fact that the surfactant which binds cooperatively to the DNA (Hayakawa et al., 1983; Shirahama et al., 1982) experiences a local phosphate concentration of at least 1.65 M suggests that the DNA molecules induce and stabilize the formation of rodlike micelles above the surfactant's cmc. It is known that collapsed DNA (Schellman & Parthasarathy, 1984; Maniatis et al., 1974) and DNA–polypeptide complexes (Azorin et al., 1985), as well as rodlike CTAB micelles at high concentrations (Ekwall, 1975), pack into a two-dimensional hexagonal symmetry. It is therefore reasonable to propose that the DNA–surfactant complex forms a two-dimensional hexagonal lattice as depicted in Figures 10 and 11.

A Model for DNA Condensation Induced by Cationic Surfactants and Anionic Polyelectrolytes. The condensation of DNA into tightly packed phases which exhibit long-range left-handed chirality requires, in addition to the cationic surfactants, a conformationally flexible anionic polymer, as evidenced by both CD and X-ray scattering measurements. The process of condensation is proposed to be the outcome of an interplay between three main interactions within the DNA–surfactant–flexible anionic polymer system. Whereas the flexible anionic polyelectrolytes stabilize close-packed clusters of spherical micelles, the relatively rigid DNA molecules are proposed to effect the elongation of the micelles into rodlike species. In addition, under conditions of charge neutralization, the DNA molecules are characterized by an intrinsic tendency to collapse and condense (Keller & Bustamante, 1986b). In order to exhibit the Ψ^- CD signals shown in Figures 1 and 2, as well as the 25-Å X-ray scattering peak, the DNA has to be packed in a manner different than that induced in the DNA–surfactant complex devoid of the flexible anionic polymer. On the basis of the strict requirement for such polymers in the DNA condensation system and following the "beads on a string" model, according to which clusters of spherical micelles represent a particularly stable form of association in the presence of the polymers, it may be suggested that the DNA-induced elongation of the micelles is arrested by these clusters, leading to the formation of capped rodlike micelles. Presumably, the specific stabilization of spherical micelles by the flexible polymers (Goddard, 1986a) makes capping less costly energetically than the elongation of the micelles induced by the DNA. As a consequence of the capping, regions of the DNA molecules are no longer surrounded by the surfactant species and, at these regions, are free to converge into the tightly packed structures which are responsible for the nonconservative ellipticities and the 25-Å scattering peak. Thus, the DNA molecules are partially embedded within the micellar organization and partially exposed to the solution environment, where Na^+ ions originating from both the DNA and the accompanying polyelectrolyte provide the minimum 90% charge neutralization required for condensation (Manning, 1980). A simplified representation of the DNA condensate and its proposed relation to the surfactant complex is depicted in Figures 12 and 13.

According to the mechanism proposed, the cationic surfactant acts as a matrix which provides the DNA molecules with a given spatial organization, a fixed directionality, and presumably, a specific handedness. The structural modulations of the prepacked DNA–surfactant complex induced by the flexible anionic polyelectrolyte allow for the convergence of the DNA strands and the final condensation. The model suggested for the packaging process is strongly supported by thhe various experimental observations. The coappearance of the 25- and 44-Å X-ray scattering peaks (Table III, Figure 9) reflecting the DNA–DNA and DNA–micelle interactions, respectively, in the case of CTAB buttresses the notion that the complex consists of DNA molecules which are partially embedded within the micellar organization and partially free to condense. It has been noted that DNA condensation is promoted by TTAB and CTAB but not by DTAB or OTAB. On the basis of the finding that no DTAB spherical micellar organization is induced by the flexible anionic polymers, it is possible that these polymers fail to modulate the DNA–DTAB complex, a situation in which the collapse and convergence of the DNA are prevented. Such a collapse cannot occur in the presence of OTAB, a surfactant that is incapable of forming spherical micelles (Lindmann & Wennerström, 1980) and therefore incapable of undergoing a rod to sphere transition. The dependence of the DNA condensation process upon the flexibility and concentration of the anionic polyelectrolyte provides additional support for the model.

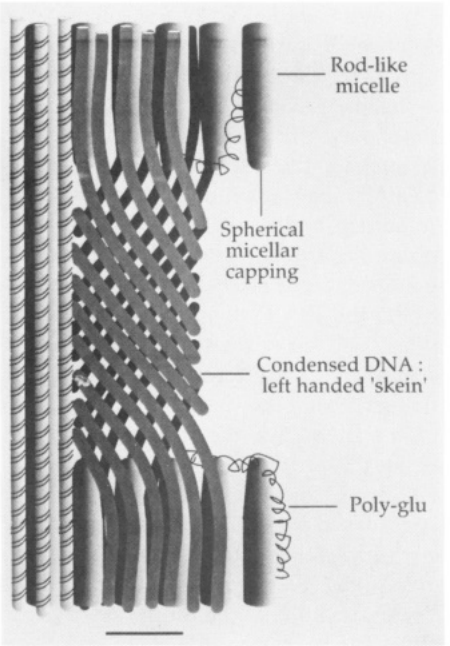

FIGURE 12: Ψ⁻-DNA condensation I: a simplified representation of the mechanism of DNA condensation within the DNA–CTAB complex, induced in the presence of the polyelectrolyte. The left-hand section of the diagram illustrates the regular DNA–CTAB hexagonal complex. The remainder highlights the rod-to-spherical micellar capping induced by the helical poly(L-Glu) shown on the right-hand side. The formation of the left-handed chiral "skein of yarn" DNA condensate is shown in the center with an exaggerated chirality. The diagram is approximately to scale with the scale bar representing 100 Å.

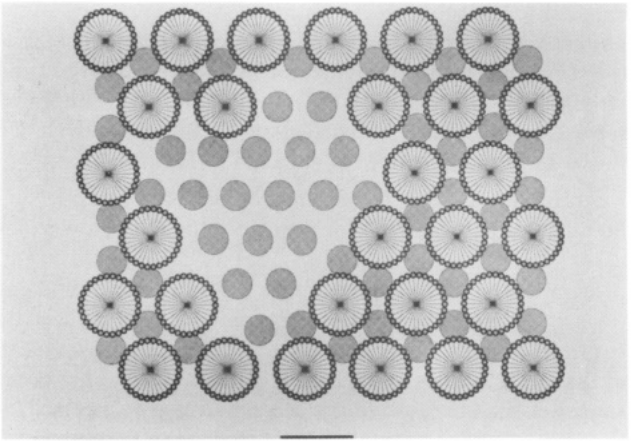

FIGURE 13: Ψ⁻-DNA condensation II: a simplified representation of the DNA condensate within the DNA–CTAB aggregate, shown in cross section. As in Figure 12, the DNA is shown as filled grey circles while the rodlike micelles are shown as an aggregate of surfactant molecules. The central area shows the DNA condensate. The diagram is approximately to scale with the scale bar representing 50 Å.

The changes observed under noncondensing conditions in the CD spectra of the DNA in the presence of TTAB and CTAB—but not in the presence of DTAB or OTAB (Figure 2)—indicate that those surfactants that promote packaging also induce *secondary conformational changes* of the DNA. We have recently been able to show that secondary conformational changes facilitate DNA packaging processes by increasing the overall elastic response of the DNA molecules (Reich et al., 1991). It is possible that such secondary conformational changes are associated with a wrapping of the DNA molecule around the rodlike micelles. Such a process is likely to depend upon the micelle's diameter (and hence is observed only for the TTAB and CTAB micelles) and to be characterized by a given handedness. The long-range left-handed organization of the condensed DNA phase, evidenced by the negative nonconservative CD signals that are obtained under all packaging conditions, may consequently be interpreted in terms of a preferential left-handed supercoiling of the DNA around the micelles which is preserved in the tightly packed DNA regions devoid of the surfactant.

A basic facet of the proposed packaging mechanism is the existence of a prepackaging phase, in which the DNA molecules are organized in a micellar scaffold. The condensation that follows the polyelectrolyte-induced capping of the rodlike micelles can consequently be regarded as an intermolecular process. The conspicuous insensitivity of the condensation to the DNA sizes and, in particular, the ability of DNA segments as short as 20 base pairs to condense indicate that the described processes are indeed intermolecular and further corroborate the proposed model.

SUMMARY

In the presence of cationic surfactants and conformationally flexible anionic polymers, DNA molecules undergo packaging into highly condensed structures that are characterized by a long-range left-handed chiral organization. The process is found to be sensitive to the type of the surfactant, being observed for TTAB and CTAB but not for DTAB or OTAB, and to depend upon the flexibility of the anionic polymers as well as upon the molar ratio between these polymers and the DNA. Within the DNA–surfactant–anionic polymer complexes, segments of the DNA molecules are tightly packed and exhibit a characteristic DNA–DNA X-ray scattering peak and nonconservative CD signals, whereas other segments are surrounded by the surfactants and reveal a DNA–surfactant scattering peak.

In order to gain insight into the DNA packaging mechanism, we have studied in a pairwise manner the anionic polymer–surfactant and the DNA–surfactant systems. The anionic polypeptides poly-Glu and poly-Asp and the single-stranded poly(A) or poly(U), but not the rigid poly(G) or double-stranded poly(A)·poly(U), induce and stabilize the clustering of spherical micelles; such an organization is observed only for micelles composed of the surfactants TTAB and CTAB. In contrast, DNA induces the formation of a micellar matrix for all the surfactants studied, namely, DTAB, TTAB, CTAB, and OTAB, resulting in DNA–surfactant complexes which reveal an X-ray scattering peak indicative of DNA–surfactant interactions. Notably, the DNA–surfactant complexes obtained in the absence of the polyelectrolytes do not reveal a DNA–DNA packing reflection or nonconservative CD signals. On the basis of these results and the known effects of a high charge density upon the micelles, the DNA–surfactant complexes obtained in the absence of the anionic polyelectrolytes were suggested to consist of closely packed rodlike micelles and DNA molecules. We propose a model in which the DNA condensation is the outcome of the interplay between the DNA-induced elongation of the micelles into rodlike aggregates and the capping of these micelles that is affected by the clusters of stabilized spherical micelles formed in the presence of the flexible anionic polymers. The capping process results in segments of the DNA that are not surrounded by the surfactant and hence are free to converge and condense. The observation that DNA condensation is induced only in the presence of TTAB and CTAB is assigned to the ability of the flexible anionic polymers to affect the organization of these particular surfactants. Thus, unlike other

condensation systems, the DNA molecules are proposed to be immobilized within a micellar matrix which acts as a prepackaging phase and determines the directionality of the helices. The very low monovalent salt concentrations required for the packaging process, as well as its insensitivity to DNA sizes, point toward the intermolecular nature of the process, a pattern that is intrinsic to the suggested model.

Various studies have indicated that a direct immobilization of DNA by membranal matrices, cellular or nuclear, is essential for in vivo processes such as DNA replication. It has been postulated that membranal structures, in conjunction with acidic proteins (McKeon et al., 1984; Adachi & Yanagida, 1989) or RNA species (Nickerson et al., 1989), are involved in the maintenance and modulation of the overall organization of DNA in biological systems. The reported in vitro condensation system, which underlies the immobilization of the DNA within a micellar matrix and the involvement of acidic polypeptides or RNA in the determination of the DNA packaging phases, point toward possible clues to processes that involve DNA–membrane interactions.

REFERENCES

Adachi, Y., & Yanagida, M. (1989) *J. Cell Biol. 108*, 1195–1207.

Arscott, P. G., Li, A.-Z., & Bloomfield, V. A. (1990) *Biopolymers 30*, 619–630.

Azorin, F., Vives, J., Campos, J. L., Jordán, A., Lloveras, J., Puigjaner, L., Subirana, J. A., Mayer, R., & Brack, A. (1985) *J. Mol. Biol. 185*, 371–387.

Barr, R. G., & Pinnavaia, T. J. (1986) *J. Phys. Chem. 90*, 328–334.

Blow, J. J., & Sleeman, A. M. (1990) *J. Cell. Sci. 95*, 383–391.

Bostock, C. J. & Sumner, A. T. (1980) in *The Eukaryotic Chromosome*, pp 180–195, North-Holland Publishing Company, Amsterdam.

Bustamante, C., Tinoco, I., & Maestre, M. F. (1983) *Proc. Natl. Acad. Sci. U.S.A. 80*, 3568–3572.

Eickbush, T. H., & Moudrianakis, E. N. (1978) *Cell 13*, 295–306.

Ekwall, P. (1975) *Adv. Liq. Cryst. 1*, 1–142.

Fendler, J. H. (1982) In *Membrane Mimetic Chemistry*, pp 6–47, John Wiley & Sons, New York.

Firshein, W. (1989) *Annu. Rev. Microbiol. 43*, 89–120.

Foe, V. E., & Alberts, B. M. (1983) *J. Cell. Sci. 61*, 31–70.

Ghirlando, R. (1991) Ph.D. Thesis, The Weizmann Institute of Science, Rehovot, Israel.

Goddard, E. D. (1986a) *Colloids Surf. 19*, 255–300.

Goddard, E. D. (1986b) *Colloids Surf. 19*, 301–329.

Hayakawa, K., Santerre, J. P., & Kwak, J. C. T. (1983) *Biophys. Chem. 17*, 175–181.

Imae, T., & Ikeda, S. (1986) *J. Phys. Chem. 90*, 5216–5223.

Imae, T., Kamiya, R., & Ikeda, S. (1985) *J. Colloid Interface Sci. 108*, 215–225.

Israelaschvili, J. N. (1985) in *Intermolecular and Surface Forces*, pp 229–275, Academic Press, New York.

Ivanov, V. I., Minchenkova, L. E., Schyolkina, A. K., & Poletayev, A. I. (1973) *Biopolymers 12*, 89–110.

Keller, D., & Bustamante, C. (1986a) *J. Chem. Phys. 84*, 2961–2971.

Keller, D., & Bustamante, C. (1986b) *J. Chem. Phys. 84*, 2972–2980.

Kim. M.-H., Ulibarri, L., Keller, D., Maestre, M. F., & Bustamante, C. (1986) *J. Chem. Phys. 84*, 2981–2989.

Lang, D. (1973) *J. Mol. Biol. 78*, 247–254.

Leno, G. H., & Lasky, R. A. (1991) *J. Cell Biol. 112*, 557–566.

Lindmann, B., & Wennerström, H. (1980) *Top. Curr. Chem. 87*, 1–83.

Maestre, M. F., & Reich, C. (1980) *Biochemistry 19*, 5214–5223.

Maniatis, T. P. (1971) Ph.D. Thesis, Vanderbilt University, Nashville, TN.

Maniatis, T., Venable, J. H., & Lerman, L. S. (1974) *J. Mol. Biol. 84*, 37–64.

Manning, G. S. (1978) *Q. Rev. Biophys. 11*, 179–246.

Manning, G. S. (1979) *Acc. Chem. Res. 12*, 443–449.

Manning, G. S. (1980) *Biopolymers 19*, 37–59.

Marquet, R., Wyart, A., & Houssier, C. (1987) *Biochim. Biophys. Acta 909*, 165–172.

McKeon, F. D., Tuffanelli, D. L., Kobayashi, S., & Kirschner, M. W. (1984) *Cell 36*, 83–92.

Morimoto, M., Ferchmin, P. A., & Bennett, E. L. (1978) *Anal. Biochem. 62*, 436–448.

Nickerson, J. A., Krochmalnic, G., Wan, K. M., & Penman, S. (1989) *Proc. Natl. Acad. Sci. U.S.A. 86*, 177–181.

Osica, V. P., Pyatigorskaya, T. L., Polyvtsev, O. F., Dembo, A. T., Klija, M. O., Vasilchenko, V. N., Venkin, B. I., & Sukharevsky, B. Ya. (1977) *Nucleic Acids Res. 4*, 1083–1096.

Ozaki, S., & Ikeda, S. (1982) *J. Colloid Interface Sci. 87*, 424–435.

Reich, Z., Ghirlando, R., & Minsky, A. (1991) *Biochemistry 30*, 7828–7836.

Riemer, S. C., & Bloomfield, V. A. (1978) *Biopolymers 17*, 785–794.

Saenger, W. (1984) in *Principles of Nucleic Acid Structure* (Cantor, C. R., Ed.), pp 368–384, Springer Verlag, New York.

Sambrook, J., Fritsch, E. F., & Maniatis, T. (1989) *Molecular Cloning. A Laboratory Manual*, 2nd Ed., Cold Spring Harbor Laboratory Press, Cold Spring Harbor, NY.

Schellman, J. A., & Parthasarathy, N. (1984) *J. Mol. Biol. 175*, 313–329.

Shelton, R. S., Van Campen, M. G., Tilford, C. H., Lang, H. C., Nisonger, L., Bandelin, F. J., & Rubenkoenig, H. L. (1946) *J. Am. Chem. Soc. 68*, 753–755.

Shinitzky, M., Dianoux, A.-C., Gitler, C., & Weber, G. (1971) *Biochemistry 11*, 2106–2113.

Shirahama, K., Masoki, T., & Takushima, K. (1982) in *Microdomains in Polymer Solution* (Dupin, P., Ed.) pp 229–310, Plenum Press, New York.

Tabony, J. (1984) *Mol. Phys. 51*, 975–989.

Wachtel, E. J., Borochov, N., & Bach, D. (1991) *Biochim. Biophys. Acta 1066*, 63–69.

Weber, G., & Bablouzian, B. (1966) *J. Biol. Chem. 241*, 2558–2561.